Journal of Engineering Science and Technology
Vol. 21, No. 3 (2026) 906 - 924

NOVEL ALKALI-TREATED GIGANTOCHLOA ALBOCILIATA AND GLASS FIBRE HYBRID COMPOSITES: EFFECTS OF FIBRE LOADING AND STACKING SEQUENCE ON MECHANICAL AND FRACTURE BEHAVIOUR

DANYAL SORAYYAEI AZAR[1], RUBENTHEREN VIYAPURI[1,*], JEFFREY C. K. L.[1], RAJKUMAR DURAIRAJ[2], S. KANNA SUBRAMANIYAN[3]

[1]Department of Mechanical and Materials Engineering, Lee Kong Chian Faculty of Engineering and Science, Universiti Tunku Abdul Rahman, Bandar Sungai Long, 43000 Kajang, Selangor, Malaysia
[2]Faculty of Engineering, Technology and Built Environment, UCSI University, UCSI Heights, 1, Jalan UCSI, Taman Connaught, 56000 Wilayah Persekutuan, Federal Territory of Kuala Lumpur, Malaysia
[3]Crashworthiness and Collision Research Group, Faculty of Mechanical and Manufacturing Engineering, Universiti Tun Hussein Onn Malaysia, Parit Raja, 86400, Malaysia
*Corresponding Author: rubentheren@utar.edu.my

Abstract

Although Malaysia hosts many bamboo species, only a small number are commercially utilised, the structural potential of *Gigantochloa albociliata* remains largely unexplored. This study investigates its suitability as reinforcement in epoxy/glass hybrid laminates by examining the effects of hybridisation, fibre loading and stacking architecture on mechanical performance and fracture behaviour. Long, continuous bamboo fibres treated in 6 wt.% sodium hydroxide for 48 hours were aligned at 0° and incorporated as a three-ply core between glass fibre skins within a sandwich configuration, fabricated across fibre loadings of 5%-20%. Tensile tests benchmarked the hybrids against neat epoxy, bamboo/epoxy and glass/epoxy laminates. The hybrid laminates delivered the highest stiffness (20.1-31.3 GPa), exceeding both bamboo-only and glass/epoxy composites. Peak strength reached 69.4 MPa at 15% fibre loading, while reduced strength at 20% was attributed to insufficient resin wetting at higher reinforcement content. Scanning electron microscope analysis confirmed effective alkali treatment through cleaner bamboo surfaces and fractography showed a progression from matrix splitting and fibre pull-out at low loading to brittle matrix cleavage and, ultimately, glass-filament fracture with bamboo pull-out at higher loading. Overall, *Gigantochloa albociliata* is demonstrated, for the first time, as a viable reinforcement for high-stiffness epoxy/glass hybrids suitable for stiffness-driven lightweight applications.

Keywords: Alkali treatment, Hybrid composite laminates mechanical performance, Sandwich structure, Scanning electron microscopy.

1. Introduction

Natural fibre composites (NFC) integrate renewable plant fibres such as bamboo, jute and flax into polymer matrices, yielding eco-friendly, lightweight materials with acceptable mechanical performance. NFCs are increasingly studied for applications in the automotive, aviation, construction and packaging sectors [1-4]. They offer advantages including low density, cost-effectiveness, biodegradability and a reduced environmental footprint compared to synthetic fibres. However, they are limited by variability in tensile strength, hydrophilicity leading to moisture uptake and poor fibre-matrix adhesion. These shortcomings cause inconsistencies in mechanical performance and restrict their wider adoption in structural applications [5-7].

A common method to address the above stated issues is to use chemical agents for treatment. Alkali treatment via NaOH is widely recognised for improving fibre-matrix interfacial bonding, as it removes amorphous constituents such as hemicellulose and lignin from NF, thereby easing stronger adhesion of the hydrophobic fibres with polymer matrices [8-11].

NaOH treatment further exposes cellulose fibrils by removing surface contaminants such as waxes and silica [12-14], while also disrupting the fibre wall through the cleavage of lignin-hemicellulose linkages [15]. These modifications increase and improve fibre surface cleanliness, promoting better resin infiltration and interfacial bonding, which in turn enhances the tensile response of alkali-treated bamboo fibres. Nevertheless, the effectiveness of this treatment has been shown to vary considerably with fibre species, immersion duration, fabrication methods and drying conditions [6, 16, 17].

Hybridization is another well-established approach for improving composite performance, where NF are combined with synthetic reinforcements such as glass fibres to produce materials with superior strength, stiffness and durability. Recent comparative work on sisal/glass/epoxy laminates demonstrated that hybridization yields significant gains in tensile and flexural strength compared to single-fibre composites, confirming that natural fibres can be successfully integrated into polymer matrices without compromising durability [18].

With earlier research on kenaf/glass hybrids, Verma et al. [19] reported tensile, and modulus increases of 68.5% and 19.5% compared to non-hybrid laminates, alongside flexural improvements of 21% and 67%. Similarly, jute/glass hybrids fabricated using hand lay-up techniques achieved tensile strengths of 71.29 MPa, significantly outperforming jute-only composites and showing improved load-bearing capacity, as reported by Pawar et al. [20].

In several studies, bamboo-glass epoxy hybrids have also proved substantial improvements with the aid of hybridization where the tensile strength has increased up to ~197 MPa and flexural strength exceeded 220 MPa, nearly doubling those of bamboo-only laminates [21]. In another research on woven laminates, the bamboo composites achieved ~115 MPa tensile strength and ~230 MPa flexural strength, with fibre orientation playing a decisive role as 0°/90° layups giving higher tensile strength, while ±45° improved modulus and shear performance [22]. Table 1 below tabulates the key findings of previous literature studies.

Across studies on bamboo-hybrid fibre composites, SEM analyses consistently revealed reduced fibre pull-out and improved fibre–matrix adhesion, confirming the effectiveness of glass reinforcement in enhancing load transfer [21-25].

Malaysia hosts over 70 bamboo species, yet only a few are commercially used [26-30]. *G. albociliata* (Malaysian honey bamboo) stays largely overlooked despite its distinctive yellow culm, high rupture strength (~181 N/mm²) that contributes to durability and dimensional stability [31, 32]. Its preliminary use in polylactic acid (PLA) composites has shown substantial performance gains (tensile strength ~19 MPa; modulus ~195 MPa versus ~2 MPa and 48 MPa for neat PLA) [33].

Its role in glass fibre-epoxy hybrids, however, has not been examined, leaving open the opportunity to establish this underutilized species as a sustainable reinforcement for advanced composite design. In addition, fibre length is a critical parameter influencing composite performance; long and continuous natural fibres ease superior stress transfer and reduce fibre pull-out compared to short fibres, due to their higher aspect ratio and fewer fibre ends acting as stress concentrators.

Prior studies on bamboo and lignocellulosic fibres confirm that tensile properties increase significantly with fibre length [34, 35]. Accordingly, this study examines the mechanical behaviour and fracture morphology of epoxy-based hybrid composites reinforced with NaOH-treated *G. albociliata* fibres and E-glass fibres, with the objective of elucidating how hybridization modifies load transfer, fibre-matrix interactions and failure mechanisms in this novel species of Malaysian bamboo.

Table 1. Comparative tensile strength results and key findings from previous studies on natural fibre/glass epoxy hybrid composites.

Study	Fibre System	Matrix	Fabrication	Tensile (MPa)	Key Finding
Verma et al. [19]	Kenaf/Glass	Epoxy	Hand lay-up	210	Hybridization improved tensile strength by 68.5%
Pawar et al. [20]	Jute/Glass	Epoxy	Hand lay-up	71.29	Improved load-bearing capacity compared to jute-only
Yudha et al. [21]	Bamboo/Glass	Epoxy	Laminate	~197	Significant tensile improvement due to hybridization
Venkatesha et al. [22]	Bamboo woven laminate	Epoxy	Layered laminate	~115	Orientation influenced strength and modulus

2. Materials and Methods

2.1. Materials

Two-year-old culms of *G. albociliata* (locally known as buluh madu or honey bamboo) were sourced from a farmer in Terengganu, found in the northern region of Malaysia. The epoxy system used was a structural grade resin (GL311-1, Part A

with Part B hardener) obtained from Penchem Malaysia. Sodium hydroxide (NaOH) pellets were supplied by Fisher Scientific and used for alkali treatment of the bamboo fibres. Silicon moulds were fabricated following ASTM D-638 standards. The E-glass fibre reinforcement was procured from MC Fibreglass & Hardware Supply, Malaysia, and supplied as continuous E-glass roving with a nominal filament diameter of 13 μm and a linear density of 2400 tex. The reported single-filament tensile strength ranged between 2400 and 3400 MPa.

2.2. Bamboo fibre treatment

Sodium hydroxide (NaOH) pellets were used to prepare an aqueous solution following a weight-to-volume ratio. Equation (1) was used to facilitate the required solution.

$$\%\frac{W}{V} = \frac{(Msolute)}{(Vsolution)} \times 100\% \quad (1)$$

A 6 wt.% NaOH solution was prepared by dissolving 180 g of pellets in distilled water under continuous stirring at approximately 65 °C. Previous studies have shown that a 6 wt.% concentration provides optimal treatment performance [8]. Continuous bamboo strips were then immersed in the solution for 48 hours at room temperature. After immersion, the fibres were rinsed thoroughly with distilled water to remove residual chemicals and surface extractives [10], followed by 24 hours of air drying. Alkali treatment durations beyond 24 hours have been reported to enhance fibre surface morphology and mechanical performance by increasing the effective bonding area between fibre and matrix [36, 37].

2.3. Critical and optimal fibre length

Before reinforcement of composites, the required reinforcement length was established following established correlations and critical-length theory. Because no direct tensile data exist for *G. albociliata*, the fibre strength was first inferred from its modulus of rupture (*MOR*) using Eq. (2). The critical length needed for effective stress transfer was then obtained from Eq. (3), and the suitability of the selected fibre length was assessed using the reinforcement criterion in Eq. (4).

$$\sigma = K \times MOR \quad (2)$$

where:

σ = Estimated fibre tensile strength (MPa),

MOR = Modulus of rupture (181 N/mm²) [31],

K = Empirical constant (0.9-1.3), here taken as 1.3.

$$L_c = (d_{avg} \times \sigma) / (2 \times \tau_c) \quad (3)$$

where:

L_c = Critical fibre length (mm),

d_{avg} = Average fibre diameter (μm),

τ_c = Matrix shear strength provided by the manufacturer.

$$L_{opt} = 30 \times Lc \quad (4)$$

where:

L_{opt} = Optimal fibre length required to ensure effective reinforcement.

Following the calculations the optimal fibre length was engineered to 12 cm to produce long and continuous fibres for more optimised stress transfer.

2.4. Preparation of mould and epoxy

Silicone moulds conforming to ASTM D-638 type III were fabricated, Fig. 1 depicts the dumbbell-shaped cavity and its dimensions (all in millimetres).

Before casting, a thin film of release agent was applied uniformly to the mould cavity. The epoxy system, Part A (resin) and Part B (hardener) was then prepared at a 4:1 ratio (epoxy: hardener) per the manufacturer's specification.

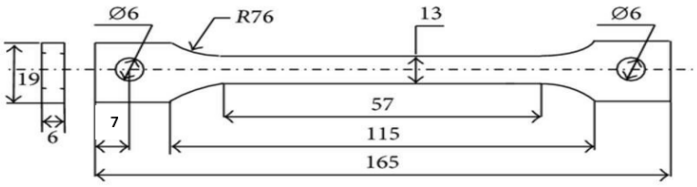

Fig. 1. ASTM D-638 III, dumbbell **mould with detailed dimensions (mm).**

2.5. Composite fabrication

Table 2 summarises the calculated material masses used to fabricate the composites at target fibre volume fractions of 5% - 20%. These values were selected with reference to prior studies indicating that NFC typically exhibit fibre contents of 20 - 40%, depending on stacking sequence and fibre geometry, as discussed by El Messiry [38]. To compute the masses in Table 2, Eqs. (5)-(7) were utilised. The volume of the composite was equal to the volume of the cavity of the mould (V_c = 25 cm^3) and constituent densities ρ_i (epoxy, glass and bamboo fibre), for each constituent i:

$$m_i = \rho_i V_c V_f^{(i)} \tag{5}$$

For hybrid laminates, the total fibre fraction $V_f^{(total)}$ was split equally between glass and bamboo:

$$V_f^{(glass)} = V_f^{(bamboo)} = 1/2\ V_f^{(total)},\ V_f^{(epoxy)} = 1\text{-}V_f^{(total)} \tag{6}$$

Epoxy was dispensed at a 4:1 resin: hardener (mass) ratio:

$$m_{resin} = 4/5\ m_{epoxy},\ m_{hardener} = 1/5\ m_{epoxy} \tag{7}$$

The computed masses were weighed during lay-up to achieve the target V_f.

Table 2. Mass of each component used for hybrid composite.

Vol%	Bamboo fibre Mass, g	E-glass Mass, g	Epoxy Mass, g	Resin Mass, g	Hardener Mass, g
5%	0.57	1.69	27.57	22.06	5.51
10%	1.14	3.38	26.12	20.90	5.22
15%	1.72	5.06	24.69	19.75	4.94
20%	2.29	6.75	23.22	18.58	4.64

Table 3 presents the fibre volume fraction compositions of the composite sample sets prepared for this study. Composite I consisted of only treated bamboo fibres with epoxy resin, while Composite II, comprised E-glass fibres with epoxy. Composite III, stood for the hybrid composites, incorporating treated bamboo fibres, E-glass fibres and epoxy resin. Each set was further divided into four fibre loadings, denoted by sample codes A-D, with the total composite volume fixed at 100%. This design enabled a systematic assessment of the influence of fibre type and V_f on the composite's tensile performance and fracture morphology.

Table 3. Composites fibre-matrix V_f % compositions.

Composite	Sample	Epoxy (V_f%)	E-glass fibre (V_f %)	Bamboo fibre (V_f %)
I	A	95	-	5
	B	90	-	10
	C	85	-	15
	D	80	-	20
II	A	95	5	-
	B	90	10	-
	C	85	15	-
	D	80	20	-
III	A	95	2.5	2.5
	B	90	5	5
	C	85	7.5	7.5
	D	80	10	10

All composites were produced using the hand lay-up technique. For the Composite I, treated bamboo fibres were aligned in a unidirectional 0° orientation and stacked layer by layer within the mould. After each layer was positioned, epoxy resin was poured to ensure full impregnation and this sequence was repeated until the mould was filled, producing a bamboo-epoxy laminate.

During lay-up, resin was gradually distributed to promote uniform wetting and minimise air entrapment. Gentle manual consolidation was applied after each layer placement, and any visible surface air bubbles were carefully removed prior to curing to reduce potential void formation. Following lay-up, a uniform light pressure was applied using a weighted press during curing to enhance laminate compaction and improve fibre–matrix interfacial contact.

For Composite III, a sandwich architecture was employed, in which E-glass skins encapsulated a bamboo fibre core. At each target fibre volume, the calculated glass fibre mass was divided equally between the two outer plies, thereby enclosing the bamboo fibre reinforcement. Like Composite I, both bamboo and E-glass fibres were arranged in a unidirectional (0°) orientation. Figure 2 depicts the configuration of the sandwich laminates. For hybrid systems (top left figure), the bamboo fibres were stacked in three layers to achieve uniform distribution across the gauge length.

Epoxy resin was introduced after each ply to ensure full wetting, with the total resin mass adjusted according to the intended fibre volume fraction (Table 3). Similar consolidation and bubble-removal procedures were implemented during fabrication of the sandwich laminates, followed by application of a light uniform

pressure during curing to minimise porosity. This process yielded a lamination sequence of {Epoxy – [E-glass fibre skin – Bamboo fibre core (3 plies) – E-glass fibre skin] – Epoxy}, designed to provide outer-layer stiffness from the glass plies and core reinforcement from the continuous bamboo fibres.

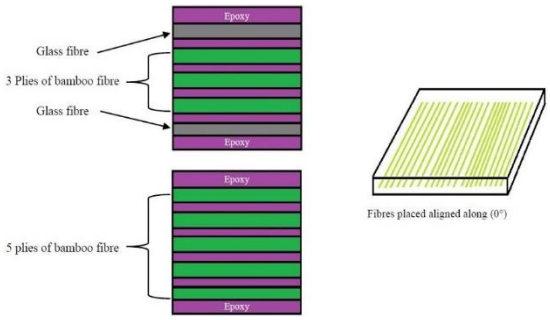

Fig. 2. Schematic of the bio and hybrid sandwich laminates with treated bamboo fibres and E-glass fibres oriented at 0°.

2.6. Tensile testing

Tensile behaviour of the composites was assessed using a Shimadzu AGS-X universal testing machine equipped with a 200 N load cell. Tests were performed at room temperature with a crosshead speed of 10 mm/min, in accordance with the specimen geometry defined in ASTM D-638 (Type III).

2.7. Morphological and fractography analysis through SEM

SEM was conducted using a HITACHI S-3400N scanning electron microscope operating at 15 kV. Prior to imaging, specimens were sputter-coated with a thin layer of Au-Pd to improve conductivity.

3. Results and Discussion

3.1. Mechanical properties of hybrid composites

The mechanical testing highlights the performance of bamboo-glass hybrid in comparison with bamboo bio-composites and E-glass/epoxy composites. The results are presented in Figs. 3-5 and summarized in Table 4.

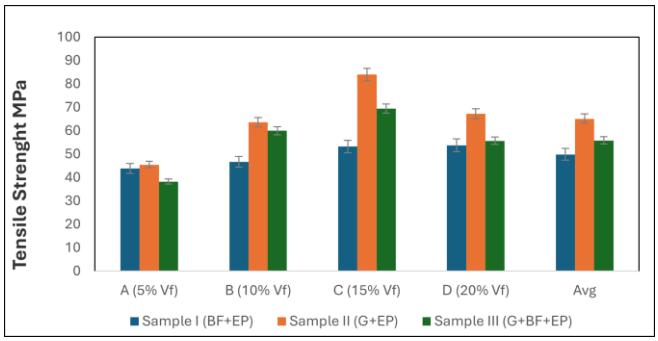

Fig. 3. Tensile strength of Composites I, II, III.

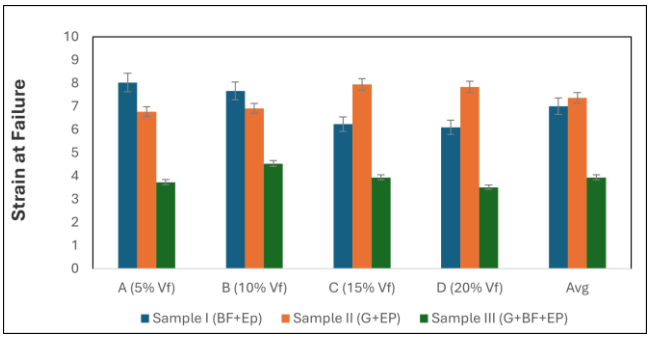

Fig. 4. Strain values at failure of Composites I, II and III.

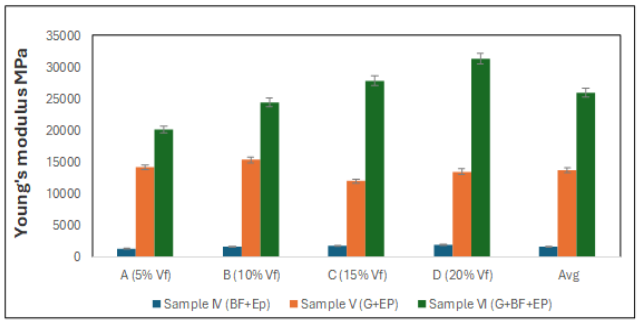

Fig. 5. Young's modulus of Composite I, II and III.

Table 4 shows that tensile strength and Young's modulus generally increase with addition of fibre content; however, in hybrid Composites III-C and III-D a decline in tensile performance is observed. This trend signals the approach of the critical fibre volume (percolation threshold), where insufficient resin wet-out and poor interfacial bonding hinder further property gains, leading to reduced tensile strength despite progressive stiffness enhancement. Similar discoveries have been reported in hybrid and filament-wound composites, where exceeding the optimum fibre content led to resin starvation and reduced strength despite rising stiffness [39, 40].

Table 4. Mechanical properties of neat epoxy, Composites I, Composite II and Composites III.

Composite	σ, MPa	ε, %	E, MPa
Neat Epoxy	**24.89**	**8.85**	**1100**
I-A	43.83	8.03	1292.6
I-B	46.66	7.66	1484.1
I-C	53.23	6.23	1653.3
I-D	53.71	6.09	1788.1
II-A	45.47	6.77	14100
II-B	63.55	6.91	15300
II-C	83.93	7.94	11900
II-D	67.25	7.84	13400
III-A	38.23	3.73	20100

III-B	59.95	4.53	24400
III-C	69.42	3.93	27800
III-D	55.62	3.51	31300

Table 5 provides average values by composite class, the keynote to be highlighted in this table is that Composite III delivered the highest average stiffness but intermediate tensile strength and reduced ductility.

Table 5. Average tensile strength, strain and modulus for composites.

Composite	Avg σ, MPa	Avg ε, %	Avg E, MPa
I	49.86	7.00	1,554.5
II	65.05	7.37	13,675
III	55.80	3.93	25,900

Table 6 highlights the average percentage of improvements relative to neat epoxy where the hybrids delivered highest value of improvement in modulus, respectively.

Table 6. Percentage improvement of average tensile strength and Young's modulus relative to neat epoxy.

Composite	% of improvement in σ	% of improvement in E
I	100.3%	41.3 %
II	161.3%	1143.2 %
III	124.1 %	2254.5%

The data from Tables 4-6 indicate that the hybrid lay-up sandwich structure effectively balances stiffness and energy absorption. This outcome is consistent with composite design principles, where combining ductile natural fibres with stiffer synthetic fibres manages the stiffness-ductility trade-off. In this case, the hybridisation of continuously oriented alkali-treated bamboo fibres with E-glass fibre reinforcement produced mechanical properties that were intermediate between the bamboo-only bio-composites (Composite I) and the glass fibre laminates (Composite II) [41].

Tensile strength results reflect this behaviour. The Composite III-C showed a 124% improvement relative to neat epoxy, although its strength remained below that of the glass fibre Composite II-C at 15% fibre loading, underscoring the dominant role of the glass layers in load bearing. The bamboo core mainly contributed to stress distribution and energy absorption. At 20% fibre loading, the reduction in tensile strength observed for Composite III-D is attributed to lower resin availability and inadequate wetting, which leads to premature fibre pull-out, a trend also noted in previous hybrid composite studies [24].

The strain results (Fig. 4 and Table 4) confirm the well-established stiffness-ductility trade-off. Composite I-A (bamboo fibre-epoxy bio-composites) reflected the greatest elongation with value of 8.03, whereas the Composite III, exhibited markedly reduced strain values across 15-20% fibre loading. This trend is consistent with findings from woven bamboo-glass hybrids, where the inclusion of stiff glass plies suppresses ductility [22, 23].

The modulus results are particularly significant. The hybrids had the highest value of modulus (31300 MPa) at 20% fibre loading which translates to a 2254.5 % increase compared with neat epoxy, surpassing the stiffness of both bamboo-only composites and glass fibre laminates. This exceptional stiffness enhancement can be attributed to the lamination sandwich structure (Fig. 2) which places E-glass on the outer layers aligned at 0°, maximising axial load transfer while the continuous bamboo fibres stabilise the laminate core.

In a related study on a different Gigantochloa species (*G. scortechinii*), Ali et al. [23] reported tensile strengths of approximately 197 MPa and flexural strengths exceeding 220 MPa for bamboo/E-glass/epoxy woven hybrids. Their results showed a similar trend to the present work: increasing the number of bamboo fibre layers in the core from two to six led to a reduction in tensile strength, although their hybrids incorporated a higher proportion of glass fibre than those examined here. While the tensile strength values in the present study are lower, largely due to differences in experimental parameters and fibre loadings, the tensile modulus of Composite III-D remains competitive at 31,300 MPa.

This enhanced stiffness arises from the use of long, continuous NaOH-treated bamboo fibres combined with E-glass reinforcement. Because these fibres exceed the critical length required for efficient stress transfer, they make a disproportionately strong contribution to the composite modulus even at comparatively lower glass content.

In contrast to the *G. albociliata*/glass sandwich hybrids developed in the present work, woven glass-dominant laminates have achieved higher tensile strengths (approximately 83-87 MPa) but at the expense of stiffness. In the study referenced, the stiffest all-glass configuration (4-ply) reached only 10.2 GPa, while mixed stacking sequences such as glass-skin/bamboo-core and bamboo-skin/glass-core produced moduli of 5.5 GPa and 1.9 GPa, respectively.

This comparison highlights an important trade-off: woven architectures prioritise tensile and flexural strength, whereas the unidirectional bamboo-core/glass-skin sandwich architecture used in this study produces stiffness values more than three times higher than those of the woven counterparts. This underscores the decisive role of stacking design in determining composite mechanical performance [21].

Glass-rich bamboo/E-glass hybrids have demonstrated substantially higher tensile strengths (150-156 MPa) and elongations of about 4.3%, but these gains in strength and ductility were accompanied by lower stiffness. In contrast, Composite III-C in the present study delivered a significantly higher modulus, showing that the unidirectional bamboo-core/glass-skin configuration favours rigidity over extensibility. This comparison highlights the trade-off between maximizing strength/strain capacity and achieving superior stiffness, with stacking architecture serving as the decisive factor in tailoring performance outcomes [22].

Yushania alpina bamboo/E-glass hybrids with a [0/90/0/90] orientation and 45% fibre loading have achieved tensile strengths ranging from 187.7 MPa for bamboo-only to 557.3 MPa for E-glass-only, with intermediate hybrids falling between 414 MPa and 534 MPa. These woven laminates also recorded elongations at break of up to 7.5% and tensile moduli in the range of 3-5 GPa. In contrast, the *G. albociliata* sandwich hybrids developed in this study exhibited lower tensile

strength and strain capacity but delivered much higher stiffness, approaching an order of magnitude greater than those woven systems. This reinforces the influence of stacking strategy on mechanical performance, as highlighted by Redda and Alene [42, 43].

Further evidence of this structural sensitivity comes from interlaminar bamboo/synthetic hybrids produced by vacuum bagging, where bamboo fabric cores were combined with outer plies of glass, carbon or aramid. Among these, the bamboo-glass configuration achieved a tensile strength of approximately 115 MPa, a modulus near 10 GPa and a strain at break of roughly 1.0%, representing a 77% strength improvement over neat bamboo (64.9 MPa). In comparison, the *G. albociliata* sandwich hybrids in the present work reached lower tensile strengths but showed higher strain capacities and an exceptional stiffness more than three times that of the woven hybrid laminate. This distinction highlights the pronounced rigidity advantage provided by the sandwich architecture [44].

A comparison with existing literature shows that the continuous 0° alignment of long, alkali-treated Malaysian honey bamboo fibres combined with E-glass skins in a sandwich lay-up provides a highly effective route for maximising stiffness while retaining moderate tensile capacity. The extended NaOH treatment improves fibre surface interfacial bonding and promotes efficient stress transfer once the critical fibre length is exceeded. This configuration therefore yields modulus values far higher than those reported for woven, interlaminar or cross-ply bamboo-glass hybrids.

Importantly, *G. albociliata* has previously been studied only at the culm scale or within PLA-based systems [33], making the present work the first to demonstrate its suitability for structural epoxy-glass hybrid composites. This contribution addresses a notable gap by positioning an underutilised Malaysian honey bamboo as a viable reinforcement for sustainable, lightweight and high-stiffness laminates. It also reinforces the broader observation that glass hybridisation reliably enhances mechanical performance while shifting the balance toward stiffness and away from ductility, reflecting a fundamental trade-off in hybrid composite design.

3.2. Morphological characteristics of treated and untreated bamboo fibres

SEM was used to examine the morphological characteristics of both untreated and NaOH-treated bamboo fibres. Figure 6 illustrates the effectiveness of the treatment, showing increased surface roughness and clearer fibre-fibril interfaces following immersion in a 6 wt.% NaOH solution for 48 hours.

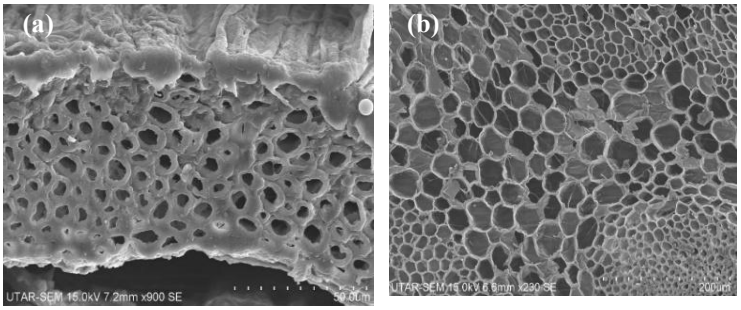

Fig. 6. SEM images of a) Untreated fibre bundles and b) 6wt. % NaOH treated fibre bundles after 48 hours.

The untreated fibres displayed a rough surface with visible impurities (Fig. 6(a)), such as waxes and other non-cellulosic materials that hinder fibre-matrix bonding. In contrast, alkali-treated fibres (Fig. 6(b)) exhibited a cleaner, more uniform structure, indicating the effective removal of these impurities. This observation aligns with earlier studies on the surface modification of bamboo fibres with treatment [8, 10, 36, 37, 45, 46].

3.3. Hybrid composites failure analysis through SEM studies

Figure 7 reveals the fractography of Composite III with fibre loading 5-20% under SEM imagery relatively from Figs. 7(a)-7(d).

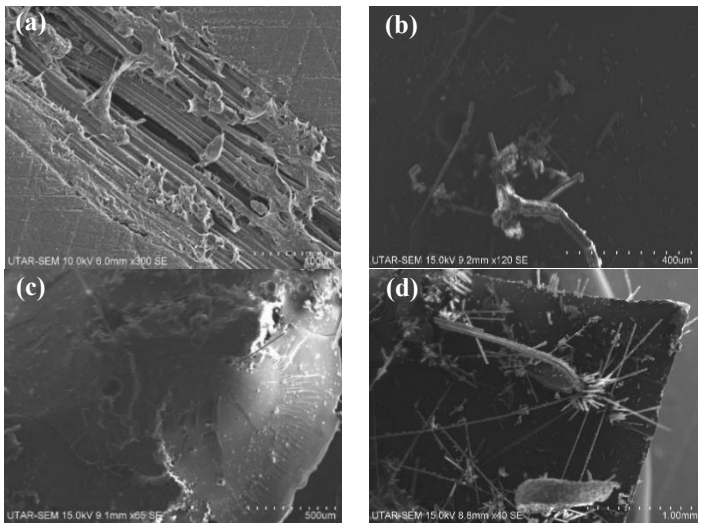

Fig. 7. SEM images of the fractured surfaces of Composite III A-D (5%-20% fibre loading), labelled respectively as (a) to (d).

Figure 7(a) represents Composite III-A, the fracture surface is matrix-rich and characterised by longitudinal splitting along the fibre axis, accompanied by pronounced fibre-matrix debonding and partial bamboo fibre pull-out. Because the glass skins are thin at this low reinforcement level, they offer limited confinement, allowing cracks to initiate within the epoxy and propagate parallel to the bamboo bundles. This morphology is typical of matrix-dominated failure, where low fibre content and weak skin restraint reduce the effectiveness of interfacial shear transfer.

Figure 7(b), show cases the surface of Composite III-B which reveals dispersed voids together with extensive bamboo fibre pull-out forming longitudinal channels and scattered glass fibre shards. The combination of porosity, pull-out and filament debris indicates interfacial debonding superimposed on matrix-dominated failure. This explains the observed property balance at this composition: stiffness rises with added reinforcement, whereas tensile strength is curtailed by void-induced stress concentrators and limited interfacial shear, allowing cracks to nucleate at pores and propagate along deboned paths rather than through cohesive fibre fracture.

In the Composite III-C (Fig. 7), a curved, mirror-like region with radiating river markings identifies brittle matrix cracking as the governing mode. Short glass-fibre

pull-out pits, filament fragments, localised epoxy debris and occasional voids are also present. Relative to Composite III-B (Fig. 7(b)), the fracture surface transitions from widespread pull-out toward more cohesive matrix cleavage with river patterns, consistent with greater fibre confinement and improved load transfer at this reinforcement level. Although both stiffness and peak strength increase, the river-patterned epoxy and residual voids confirm that matrix cracking remains dominant, with interfacial debonding acting as a secondary mechanism, the river markings trace crack initiation near the edge and subsequent propagation across the laminate.

In Composite III-D (Fig. 7(d)), the sandwich morphology is pronounced: the glass skins contain fractured E-glass filaments with many short-broken ends embedded in the epoxy, while the bamboo fibre core exhibited long pull-out and interfacial debonding. Epoxy debris is widespread, voids are scarce, and hairline cracks appear near the fracture boundary. This combination indicates effective load transfer into the glass skins (evidenced by filament breakage rather than long pull-out) but a comparatively weaker bamboo/epoxy interface.

At this high total fibre fraction, the matrix becomes locally insufficient for wetting and crack blunting, enabling early microcrack nucleation at edges and interfaces. Consequently, Composite III-D exhibits the expected property split-highest modulus from the increased stiff-fibre fraction and skins-in-sandwich architecture, but lower tensile strength than Composite III-C (Table 4) due to interface-controlled failure and limited matrix capacity to arrest cracks.

Taken together, the fracture sequence in Composite III from A to D shows a clear evolution with increasing reinforcement. At low fibre loadings (5% and 10%), failure is dominated by matrix-driven splitting and bamboo pull-out. At intermediate levels, the morphology transitions to brittle matrix cleavage marked by river patterns. At the highest reinforcement, failure shifts toward glass-filament fracture in the skins accompanied by bamboo pull-out in the core.

This microstructural progression aligns with the mechanical response: stiffness increases consistently with fibre content, while tensile strength reaches a maximum at Composite III-C before declining at Composite III-D as the laminate approaches a critical fibre-volume regime where matrix and interfacial constraints begin to control failure.

The failure morphologies observed in Composite III agree closely with trends reported in earlier bamboo-glass hybrid studies. Yudha et al. by investigation on the role of bamboo and glass fibres in hybrid composites [21] found that, bamboo-rich laminates exhibited voids, smooth deboned regions and extensive fibre pull-out due to weak interfacial adhesion, consistent with the matrix-dominated splitting and pull-out seen in Composites III-A and III-B.

Glass-dominant laminates in the same study showed filament breakage and matrix debris adhering to fibre surfaces, indicating stronger fibre-matrix bonding; this corresponds to the fractured E-glass filaments observed in Composite III-D, where load transfer into the skins is efficient.

Similar features were noted by Venkatesha et al. [22], where fibre pull-out, breakage and delamination governed tensile failure in hybrid bamboo woven laminates. These behaviours parallel the mixed pull-out and brittle cleavage seen in Composite III-B and III-C. The influence of bamboo content reported by Ali et al. [23] on *G. scortechinii* bamboo fibre with E-glass/epoxy hybrid composites also

matches the present findings: increasing bamboo layers promoted void formation, poor bonding and reduced impact/tensile performance, comparable to the transition from Composite III-C to III-D where higher fibre volumes restricted resin wetting and intensified debonding.

Overall, the SEM trends in this study align well with established bamboo-glass hybrid behaviour, while the pronounced glass-filament fracture and high stiffness at elevated fibre fractions reflect the specific unidirectional sandwich architecture used here.

4. Conclusions

This study shows that sandwich laminates combining long, continuous 48-hour NaOH-treated *G. albociliata* fibres with 0° E-glass skins provide a substantial stiffness advantage while maintaining moderate tensile capacity. Across the fibre loading range of 5-20 percent, the hybrid configuration achieved a maximum Young's modulus of 31.3 GPa at 20% loading (Composite III-D) and a peak tensile strength of 69.4 MPa at 15% loading (Composite III-C). These values exceed those of bamboo-only bio-composites in stiffness and approach the strength levels of glass/epoxy laminates.

Fractography revealed a clear progression in failure mechanisms: matrix-dominated splitting and fibre pull-out at low reinforcement Composites (III-A, III-B), brittle matrix cleavage with river markings at intermediate loading (Composite III-C) and glass-filament fracture in the skins coupled with bamboo pull-out in the core at high reinforcement (Composite III-D). This sequence reflects the expected stiffness ductility trade-off in hybrid laminates, where skins-dominated load paths elevate modulus but restrict strain to failure.

The findings establish *G. albociliata* Malaysian honey bamboo as a viable reinforcement for epoxy-glass hybrid composites, marking the first demonstration of its potential in structural hybrid systems. Composite III-C offers a balanced property profile (≈69 MPa tensile strength; 27.8 GPa modulus) suitable for applications requiring moderate strength with high axial rigidity, while Composite III-D is suited to stiffness-critical designs, with the acknowledged limitation of reduced strength and ductility due to resin insufficiency at higher fibre loading.

Overall, the continuous-fibre, skins-dominated sandwich architecture employed here provides an effective route to high-stiffness, lightweight hybrid composites and highlights the potential of an underutilised Malaysian bamboo species for sustainable structural applications.

In practical terms, the tensile stiffness and strength levels achieved suggest suitability for lightweight secondary structural components where axial rigidity and weight reduction govern design priorities, such as non-primary casings, protective shells, and structural covers in engineering assemblies. When considered alongside complementary thermal and crystallinity investigations conducted on *G. albociliata*-based hybrid systems, the present mechanical findings further reinforce the material's viability for sustainable hybrid composite development.

Acknowledgement

This research was done under the auspices of Centre for Railway Infrastructure and Engineering at the Lee Kong Chian Faculty of Engineering and Science, Universiti

Tunku Abdul Rahman, Sungai Long, Malaysia. It is primarily funded by UTARRF Grant IPSR/RMC/UTARRF/2021-C2/R0.

Nomenclatures

Composite I	Bamboo fibre/epoxy composite
Composite II	E-glass fibre/epoxy composite
Composite III	Bamboo fibre/E-glass fibre/epoxy composite
d_{avg}	Average fibre diameter (μm)
E	Young's modulus (MPa or GPa, as specified)
k	Empirical factor relating σ and MOR
L_c	Critical fibre length (mm)
L_{opt}	Optimal fibre length for effective reinforcement (mm)
m_i	Mass of constituent *i* (g)
MOR	Modulus of rupture (N/mm²)
M_{solute}	Mass of solute (g)
V_c	Volume of composite / mould cavity (cm³)
V_f	Fibre volume fraction
$V_{f(i)}$	Fibre volume fraction of constituent *i*
$V_{solution}$	Volume of solution (cm³)

Greek Symbols

ε	Strain at break (%)
ρ_i	Density of constituent i (g/cm³)
σ	Tensile strength (MPa)
τ_c	Matrix shear strength (MPa)

Abbreviations

ASTM	American Society for Testing and Materials
Au-Pd	Gold–palladium coating
G. albociliata	Gigantochloa albociliata
G. scortechinii	Gigantochloa scortechinii
GPa	Gigapascal
MPa	Megapascal
NaOH	Sodium hydroxide
NF	Natural fibre(s)
NFC	Natural fibre composite(s)
PLA	Poly (lactic acid)
SEM	Scanning electron microscopy
wt.%	Weight percent

References

1. Prasad, V.; Alliyankal Vijayakumar, A.; Jose, T.; and George, S.C. (2024). A comprehensive review of sustainability in natural-fiber-reinforced polymers. *Sustainability*, 16(3), 1223.
2. Puttegowda, M. (2025). Eco-friendly composites: Exploring the potential of natural fiber reinforcement. *Discover Applied Sciences*, 7(5), 401.
3. Pokharel, A.; Falua, K.J.; Babaei-Ghazvini, A.; and Acharya, B. (2022). Biobased polymer composites: A review. *Journal of Composite Science*, 6(9), 255.

4. Ares Elejoste, P.; Seoane-Rivero, R.; Neira Hernandez, S.; Iturmendi Aguirrebeitia, A.; and Gondra Zubieta, K. (2023). Analysis of the advances in the development of new generation of sustainable, bio-based and/or recyclable composites. *DYNA*, 98(1), 7-9.
5. Al-Azad, N.; Asril, M.F.M.; and Shah, M.K.M. (2021). A review on development of natural fibre composites for construction applications. *Journal of Materials Science and Chemical Engineering*, 9(07), 1-9.
6. Kamarudin, S.H.; Mohd Basri, M.S.; Rayung, M.; Abu, F.; Ahmad, S.; Norizan, M.N.; Osman, S.; Sarifuddin, N.; Desa, M.S.Z.M.; Abdullah, U.H.; Mohamed Amin Tawakkal, I.S.; and Abdullah, L.C. (2022). A review on natural fiber reinforced polymer composites (NFRPC) for sustainable industrial applications. *Polymers*, 14(17), 3698.
7. Islam, T.; Chaion, M.H.; Jalil, M.A.; Rafi, A.S.; Mushtari, F.; Dhar, A.K.; and Hossain, S. (2024). Advancements and challenges in natural fiber-reinforced hybrid composites: A comprehensive review. *SPE Polymers*, 5(4), 481-506.
8. Asmare, F.W.; Liu, X.; Qiao, G.; Li, R.; Babu K, M.; and Wu, D. (2024). Investigation and application of different extraction techniques for the production of finer bamboo fibres. *Advances in Bamboo Science*, 7, 100070.
9. Hamidon, M.H.; Sultan, M.T.H.; Ariffin, A.H.; and Shah, A.U.M. (2019). Effects of fibre treatment on mechanical properties of kenaf fibre reinforced composites: A review. *Journal of Materials Research and Technology*, 8(3), 3327-3337.
10. Abdullah, N.A.; and Hashim, M.Y. (2022). Effect of tensile strength on treated bamboo fiber with alkali treatment compared to untreated bamboo fiber. *Research Progress in Mechanical and Manufacturing Engineering*, 3(1), 393-402.
11. Kudva, A.; G T, M.; and Pai, D. (2024). Influence of chemical treatment on the physical and mechanical properties of bamboo fibers as potential reinforcement for polymer composites. *Journal of Natural Fibers*, 21(1), 2332698.
12. Geremew, A.; De Winne, P.; Demissie, T.A.; and De Backer, H. (2024). Surface modification of bamboo fibers through alkaline treatment: Morphological and physical characterization for composite reinforcement. *Journal of Engineered Fibers and Fabrics*, 19, 1-13.
13. Widodo, E.; Pratikto; Sugiarto; and Widodo, T.D. (2024). Comprehensive investigation of raw and NaOH alkalized Sansevieria fiber for enhancing composite reinforcement. *Case Studies in Chemical and Environmental Engineering*, 9, 100546.
14. Maguteeswaran, R.; Prathap, P.; Satheeshkumar, S.; and Madhu, S. (2024). Effect of alkali treatment on novel natural fiber extracted from the stem of Lankaran acacia for polymer composite applications. *Biomass Conversion and Biorefinery*, 14(6), 8091-8101.
15. Chen, X.; Wang, X.; Gu, S.; Huang, A.; and Cheng, H. (2025). Effects of alkali treatment on the bending and fracture behavior of biomaterial bamboo. *Polymer Testing*, 143, 108715.
16. Seisa, K.; Chinnasamy, V.; and Ude, A.U. (2022). Surface treatments of natural fibres in fibre reinforced composites: A review. *Fibres and Textiles in Eastern Europe*, 151(2), 82-89.

17. Bai, Y.; Wang, W.; Zhang, Y.; Wang, X.; Wang, X.; and Shi, J. (2022). Effects of different delignification and drying methods on fiber properties of Moso bamboo. *Polymers*, 14(24), 5464.
18. Rudresh, M.; Prathik Jain, S.; Dinamani Muthaiah; Bhargav Yadav, L.; Diwakar, S.S.; Sumantha Upadhyaya, K.S.; and Yogesh, V. (2025). Comparative study of mechanical properties of sisal/epoxy, fiber/glass epoxy, sisal/fiber glass/epoxy composites. *Journal of Polymer and Composites*, 13(03), 1-11.
19. Verma, R.; Shukla, M.; and Shukla, D.K. (2022). Effect of glass fiber hybridization on the mechanical properties of unidirectional, alkali treated kenaf epoxy composites. *Polymer Composites*, 43(10), 7483-7499.
20. Pawar, U.S.; Chavan, S.S.; and Mohite, D.D. (2024). Synthesis of glass FRP natural fiber hybrid composites (NFHC) and its mechanical characterization. *Discover Sustainability*, 5(1), 44.
21. Yudha, N.K.; Nugroho, A.D.; Erlangga, W.; Jamasri; Fiedler, B.; and Muḥikhun, M.A. (2025). Sustainable high-performance materials: The role of bamboo and glass fibers in hybrid composites. *Hybrid Advances*, 9, 100416.
22. Venkatesha, B.K.; Saravanan, R.; and Saravana Bavan, D. (2018). Mechanical properties of woven bamboo/E-glass fiber reinforced epoxy hybrid composites. *International Journal of Mechanical and Production Engineering Research and Development* (*IJMPERD*), Special Issue, 57-66.
23. Ali, A.; Rassiah, K.; and Ahmad, M.M.H.M. (2021). Mechanical characterization of Gigantochloa scortechinii bamboo fiber with E-glass/epoxy hybrid composites. *Journal of Southwest Jiaotong University*, 56(3), 96-110.
24. Islam, M.A.; Islam, M.; Islam, M.S.; and Islam, T. (2025). Enhanced properties of bamboo short fiber reinforced polymer composites with alkali and graphene oxide. *Materials Advances*, 6(14), 4738-4754.
25. Ahmad, S.M.; M C, G.; Shettar, M.; and Sharma, S. (2023). Experimental investigation of mechanical properties and morphology of bamboo-glass fiber-nanoclay epoxy hybrid composites. *Cogent Engineering*, 10(2), 2279209.
26. Hassan, N.H.M.; Abdullah, N.; Kelana, D.N.A.; and Perumal, M. (2022). Early field growth performance of ten selected bamboo taxa: The case study of Sabal Bamboo Pilot Project in Sarawak, Malaysia. *Biodiversitas Journal of Biological Diversity*, 23(6), 2882-2892.
27. Jarawi, N.; and Jusoh, I. (2023). Charcoal properties of Malaysian bamboo charcoal carbonized at 750 °C. *BioResources*, 18(3), 4413-4429.
28. Hawanis, H.S.N.; and Ilyas, R.A. (2022). Bamboo species and utilization in Malaysia: A mini review. *Proceedings of the Composite Sciences and Technology International Conference* 2022 (*COMSAT* 2022), Johor Bahru, Malaysia., 1-3.
29. Correal, F.F. (2020). *Bamboo design and construction*. In Harries, K.A.; and Sharma, B. (Eds.), *Nonconventional and Vernacular Construction Materials*. Elsevier, 521-559.
30. Forestry Department of Peninsular Malaysia. (2022). Bamboo and rattan. Retrieved September 5, 2025, from https://www.forestry.gov.my/en/buluh-dan-rotan.

31. Kasdi, S.A.; Lee, S.H.; Md. Tahir, P.; al-Edrus, S.S.O.; Salim, S.; Abd Ghani, M.A.; Bakar, B.F.A.; Lum, W.C.; and Zhang, J. (2023). Characterization of the properties of Buluh Madu (Gigantochloa albociliata). *BioResources*, 18(4), 8503-8514.
32. Yusoff, M.S.R.; Bahari, S.A.; Haliffuddin, R.M.A.A.; Zakaria, M.N.; Jamaluddin, M.A.; and Rashid, N.H.M.N. (2021). Chemical contents and thermal stability of Madu bamboo (Gigantochloa albociliata) for natural bonded fiber composites. *IOP Conference Series*: *Earth and Environmental Science*, 644(1), 012009.
33. Mohktar, N.Q.; Ahmad, M.; and Masrol, S.R. (2023). Characterization and tensile properties of silane treated bamboo fibre reinforced poly (lactic) acid composite. *Progress in Engineering Application and Technology*, 4(1), 51-59.
34. Sajin, J.B.; Christu Paul, R.; Binoj, J.S.; Brailson Mansingh, B.; Gerald Arul Selvan, M.; Goh, K.L.; Rimal Isaac, R.S.; and Senthil Saravanan, M.S. (2021). Impact of fiber length on mechanical, morphological and thermal analysis of chemical treated jute fiber polymer composites for sustainable applications. *Current Research in Green and Sustainable Chemistry*, 5, 100241.
35. Nagaraja, S.; Anand, P.B.; K., M.K.; and Ammarullah, M.I. (2024). Synergistic advances in natural fibre composites: A comprehensive review of the eco-friendly bio-composite development, its characterization and diverse applications. *RSC Advances*, 14, 17594-17611.
36. Gouda, K.; Bhowmik, S.; and Das, B. (2020). Thermomechanical behavior of graphene nanoplatelets and bamboo micro filler incorporated epoxy hybrid composites. *Materials Research Express*, 7(1), 015328.
37. Chin, S.C.; Tee, K.F.; Tong, F.S.; Ong, H.R.; and Gimbun, J. (2020). Thermal and mechanical properties of bamboo fiber reinforced composites. *Materials Today Communications*, 23, 100876.
38. El Messiry, M. (2013). Theoretical analysis of natural fiber volume fraction of reinforced composites. *Alexandria Engineering Journal*, 52(3), 301-306.
39. Wang, Q.; Li, T.; Wang, B.; Liu, C.; Huang, Q.; and Ren, M. (2020). Prediction of void growth and fiber volume fraction based on filament winding process mechanics. *Composites Structures*, 246, 112432.
40. Wang, A.; Yang, Y.; Zhang, P.; Liu, X.; and Xu, G. (2024). Effect of fiber volume fraction on hybrid effects of tensile properties of unidirectional aramid/carbon fiber hybrid composites. *Polymer Composites*, 45(3), 2050-2062.
41. Ikbal, M.H.; Ahmed, A.; Qingtao, W.; Shuai, Z.; and Wei, L. (2017). Hybrid composites made of unidirectional T600S carbon and E-glass fabrics under quasi-static loading. *Journal of Industrial Textiles*, 46(7), 1511-1535.
42. Praveen Kumar, K.; Sridhar, B.; Ramakrishna, C.; Hemanth, M.; Shiva Shankar Chary, V.; Jyothi, V.; and Kumar, M. (2024). Mechanical characterization of bamboo and glass fiber hybrid composite material. *MATEC Web of Conferences*, 392, 01015.
43. Redda, D.; and Alene, A. (2016). Experimental analysis of bamboo and E-glass fiber reinforced epoxy hybrid composite. *Journal of Materials Science and Engineering B*, 6(5-6), 153-160.

44. Oliveira, M.; Neves, V.; and Banea, M.D. (2024). Mechanical and thermal characterization of bamboo and interlaminar hybrid bamboo/synthetic fibre-reinforced epoxy composites. *Materials*, 17(8), 1777.
45. Zhang, K.; Wang, F.; Liang, W.; Wang, Z.; Duan, Z.; and Yang, B. (2018). Thermal and mechanical properties of bamboo fiber reinforced epoxy composites. *Polymers*, 10(6), 608.
46. Kaima, J.; Preechawuttipong, I.; Peyroux, R.; Jongchansitto, P.; and Kaima, T. (2023). Experimental investigation of alkaline treatment processes (NaOH, KOH and ash) on tensile strength of the bamboo fiber bundle. *Results in Engineering*, 18, 101186.